Journal of Alloys and Compounds 504 (2010) 559–565

Contents lists available at ScienceDirect

Journal of Alloys and Compounds

journal homepage: www.elsevier.com/locate/jallcom

# Structural, electronic, optical and thermal properties of $Al_xGa_{1-x}As_ySb_{1-y}$ quaternary alloys: First-principles study

F. El Haj Hassan[a,b,*], A.V. Postnikov[c], O. Pagès[c]

[a] Université Libanaise, Faculté des sciences (I), Laboratoire de Physique de Matériaux, Elhadath, Beirut, Lebanon
[b] Condensed Matter Section, the Abdus Salam International Centre for Theoretical Physics (ICTP), Strada Costiera 11, 34014 Trieste, Italy
[c] Laboratoire de Physique des Milieux Denses, Université Paul Verlaine—Metz, 1 Bd. Arago, 57078 Metz, France

ARTICLE INFO

*Article history:*
Received 10 March 2010
Received in revised form 21 May 2010
Accepted 29 May 2010
Available online 11 June 2010

*Keywords:*
FP-LAPW
DFT
Quaternary alloys
Band structures
Dielectric function

*PACS:*
61.66.Dk
71.15.Ap
71.15.Mb
71.20.−b
77.22.Ch

ABSTRACT

First-principles calculations are performed to study the structural, electronic, optical and thermodynamic properties of technologically important $Al_xGa_{1-x}As_ySb_{1-y}$ quaternary alloys using the full potential-linearized augmented plane wave plus local orbitals method within the density functional theory. We use both Wu–Cohen and Engel–Vosko generalized gradient approximations of the exchange-correlation energy that are based on the optimization of total energy and corresponding potential, respectively. Our investigation on the effect of composition on lattice constant, bulk modulus and band gap for pseudobinary as well as for quaternary alloys shows nonlinear dependence on the composition. The bowing of the fundamental gap versus composition predicted by our calculations is in very good agreement with experiments available for pseudobinary alloys. The presented contour maps of energy band gap and lattice constants versus concentrations could be very useful for designing new structures with desired optical properties. In addition, the energy band gap and natural band offset of zinc-blende $Al_xGa_{1-x}As_ySb_{1-y}$ quaternary alloys lattice matched to GaSb and InAs substrates is investigated. The obtained results show that the quaternary alloys of interest could be appropriate materials for designing heterostructures with desired optical and interfacial properties.



## 1. Introduction

The capabilities of III–V quantum well devices can frequently be expanded by introducing quaternary layers to the design. This increased flexibility does, however, come at the expense of a more difficult growth coupled with the need for multiple tedious calibration runs to accurately fix the composition. A major requirement for optoelectronic applications of materials is the ability to tune independently the band gap – to realize the desired optical properties – and the lattice parameter – in order to be able to match it on a given substrate [1,2].

The $Al_xGa_{1-x}As_ySb_{1-y}$ semiconductor alloys cover a wide spectral range of wavelengths between the visible region and infrared region (0.57–1.72 μm) [3] and thus are promising for many device applications such as injection lasers [4,5], photodiodes [6], and solar cells [7]. The $Al_xGa_{1-x}As_ySb_{1-y}$ alloys are also interesting materials for cladding layers of the GaInAsSb/AlGaAsSb injections lasers [8,9]. The alloys can be grown lattice matched to commercially available binary substrates GaSb [10] and InAs [11].

The quaternary compounds $Al_xGa_{1-x}As_ySb_{1-y}$ are bordered by the ternary alloys $Al_xGa_{1-x}As$, $Al_xGa_{1-x}Sb$, $GaAs_xSb_{1-x}$ and $AlAs_xSb_{1-x}$ which are studied recently by our group [12].

The theoretical work carried out on the $Al_xGa_{1-x}As_ySb_{1-y}$ quaternary alloys was so far limited by computational difficulties associated with the alloy disorder. The band gap of $Al_xGa_{1-x}As_ySb_{1-y-y}$ was estimated using the interpolation [13,14] scheme and the correlated function expansion [15] (CFE) methodology. The effects of structural and chemical disorder on the electronic properties were studied on the basis of tight-binding theory [16]. The elastic properties were calculated using pseudopotential empirical method (EPM) [17].

In order to complete the existing experimental and theoretical works and to provide a basis for understanding future device concepts and applications, we have employed density functional theory (DFT) to study the structural, electronic, optical and thermodynamic properties of $Al_xGa_{1-x}As_ySb_{1-y}$ quaternary alloys. First, the lattice constant parameter, the bulk modulus, the band gap energy, the refractive index, the Debye temperature, the heat

* Corresponding author at: Université Libanaise, Faculté des sciences (I), Laboratoire de Physique de Matériaux, Elhadath, Beirut, Lebanon.
Tel.: +961 5 460494; fax: +961 5 461496.
*E-mail address:* hassan.f@ul.edu.lb (F.E.H. Hassan).

0925-8388/$ – see front matter © 2010 Elsevier B.V. All rights reserved.
doi:10.1016/j.jallcom.2010.05.161

**Table 1**
Calculated lattice parameter $a$, bulk modulus $B$, and gap energy $E_g$ for the binary compounds in zinc-blende structure at equilibrium volume. Experimental data are also shown for comparison. (Ours: this work; WC: Wu and Cohen GGA; PBE: Perdew–Burke–Ernzerhof GGA; EV: Engel–Vosko GGA).

| | $a$ (Å) | | | $B$ (GPa) | | | $E_g$ (eV) | | |
|---|---|---|---|---|---|---|---|---|---|
| | Our work | | Exp. | Our work | | Exp. | Our work | | Exp. |
| | WC | PBE | | WC | PBE | | WC | EV | |
| GaAs | 5.666 | 5.754 | 5.653[a] | 69.6 | 60.9 | 75.5[a] | 0.336 | 0.966 | 1.424 ($E_g^{\Gamma}$)[a] |
| GaSb | 6.115 | 6.221 | 6.096[a] | 51.9 | 45.9 | 56.3[a] | 0.000 | 0.396 | 0.726 ($E_g^{\Gamma}$)[a] |
| AlAs | 5.678 | 5.736 | 5.661[a] | 72.3 | 66.8 | 78.1[a] | 1.861 | 2.104 | 2.170 ($E_g^{X}$)[a] |
| AlSb | 6.160 | 6.232 | 6.135[b] | 54.9 | 49.7 | 55.1[c] | 1.343 | 1.470 | 1.696 ($E_g^{X}$)[b] |
| | | | 6.058[a] | | | 58.0[d] | | | 0.417 ($E_g^{\Gamma}$)[b] |

[a] Ref. [13].
[b] Ref. [29].
[c] Ref. [30].
[d] Ref. [31].

capacity and the thermal expansion coefficient were found to vary in additive way in what regards their dependences on cationic and anionic compositions ($x$, $y$). Second, the energy band gap, natural band offset, optical and thermal properties of zinc-blende $Al_xGa_{1-x}As_ySb_{1-y}$ quaternary alloys lattice matched to GaSb and InAs substrate have been investigated.

The paper is organized as follows: in Section 2, we describe the computational details; results and discussions concerning the binary compounds as well as the ternary and quaternary alloys are presented in Section 3; the paper is concluded in Section 4.

## 2. Computational details

Describing random alloys by periodic structures will clearly introduce spurious correlations beyond certain distance. Preventing this problem needs a very large supercell for which first-principle self-consistent calculations are still impractical. However, many physical properties of solids are characterized by microscopic length scales and local randomness of alloys so that modifying the large scale randomness of alloys does not affect these properties. Zunger et al. [18] implemented this fact to construct *Special Quasirandom Structures* (SQS) approach by close reproduction of the perfectly random network for the first few shells around a given site, deferring periodicity errors to more distant neighbors. Such an approach somehow justifies a use of specially designed supercells, whose size remains the user's choice, for the study of certain properties of random alloys. As the limiting case, we use in the present study the minimal supercells compatible with the percentage of constituents in question. The lattice structures of the ternary alloys have been modeled at some selected compositions $x = 0.25$, 0.5, 0.75. For the considered structures, we perform the structural optimization by minimizing the total energy with respect to the cell parameters and also the atomic positions. For the compositions $x = 0.25$ and 0.75 the simplest structure is an eight-atom simple cubic cell (luzonite): the anions with the lower concentration form a regular simple cubic lattice. For the composition $x = 0.5$, the smallest ordered structure is a four-atom tetragonal cell, corresponding to the (0 0 1) superlattice. This structure is strongly anisotropic, and thus not very suitable for simulating random alloys which are macroscopically isotropic. We consider therefore the chalcopyrite structure, which has a 16-atom tetragonal cell.

We have employed the scalar-relativistic FP-LAPW + lo method [19–21] within the framework of DFT [22,23] as implemented in WIEN2K [24] code. For structural properties the exchange-correlation potential was calculated using the generalized gradient approximation (GGA) in the new form (WC) proposed by Wu and Cohen [25] which is a improved form of the most popular Perdew–Burke–Ernzerhof (PBE) GGA [26]. In addition, and for electronic properties only, we applied the Engel–Vosko (EV) scheme [27]. In the FP-LAPW + lo method, the wave function, charge density and potential were expanded by spherical harmonic functions inside non-overlapping spheres surrounding the atomic sites (muffin-tin spheres) and by plane waves basis set in the remaining space of the unit cell (interstitial region). A mesh of 35 special $k$ points for binary compounds, 27 special $k$ points for ternary alloys, and 32 special $k$ points for quaternary alloys were taken in the irreducible wedge of Brillouin zone. The maximum $l$ quantum number for the wave function expansion inside atomic spheres was confined to $l_{max} = 10$. The plane wave cutoff of $K_{max} = 8.0/R_{MT}$ ($R_{MT}$ is the smallest muffin-tin radius in the unit cell) is chosen for the expansion of the wave functions in the interstitial region while the charge density is Fourier expanded up to $G_{max} = 14(Ryd)^{1/2}$. The muffin-tin radius was assumed to be 2.0, 2.1, 2.2 and 2.3 a.u. for Al, Ga, As and Sb atoms, respectively. Both the plane wave cutoff and the number of $k$-points were varied to ensure total energy convergence. Our calculations for valence electrons were performed in a scalar-relativistic approximation, with neglecting spin-orbit coupling, while the core electrons were treated fully relativistic.

## 3. Results and discussion

The quaternary compounds $Al_xGa_{1-x}As_ySb_{1-y}$ are bordered by the ternary alloys $Al_xGa_{1-x}As$, $Al_xGa_{1-x}Sb$, $GaAs_xSb_{1-x}$ and $AlAs_xSb_{1-x}$ which are bounded, in their turn, by four binary compounds (GaSb, GaAs, AlSb, and AlAs). Before handling the main steps of the present work, let us start with a preliminary study of the structural and electronic properties of the binary compounds GaSb, GaAs, AlSb, and AlAs which crystallize in the two-atom unit cell zinc-blende lattice structure. The calculated total energies using GGA scheme at many different volumes around equilibrium were fitted by Murnaghan's equation-of-state [28]. The equilibrium lattice parameter, bulk modulus and gap energy were presented and compared with the experimental data in Table 1. In addition, the properties of InAs, which is one of the zinc-blende compounds lattice matched with the alloys, were added to the same Table. It is clearly seen that the WC calculated lattice constants and bulk modulus are more accurate than those of PBE. A small difference (less than 1%) could be observed between WC calculated and experimental lattice constants which can be attributed to the general trend that GGA usually overestimates these parameters [32,33].

The computed band structures of binary compounds using WC and EV schemes indicate a direct band gap for GaAs and GaSb, while AlAs and AlSb are an indirect band gap with the X-L-Γ ordering of the conduction valley minima. In fact, GGA usually underestimates the experimental energy band gap [34–36], this is an intrinsic feature of DFT which is not suitable for describing excited-state properties. However, it is widely accepted that GGA electronic band

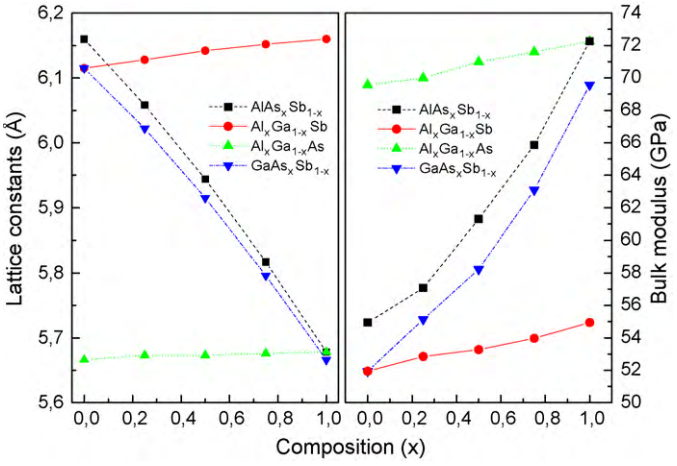


**Fig. 1.** Composition dependence of the calculated lattice constant (left panel) and bulk modulus (right panel) of the four ternary alloys using WC-GGA.

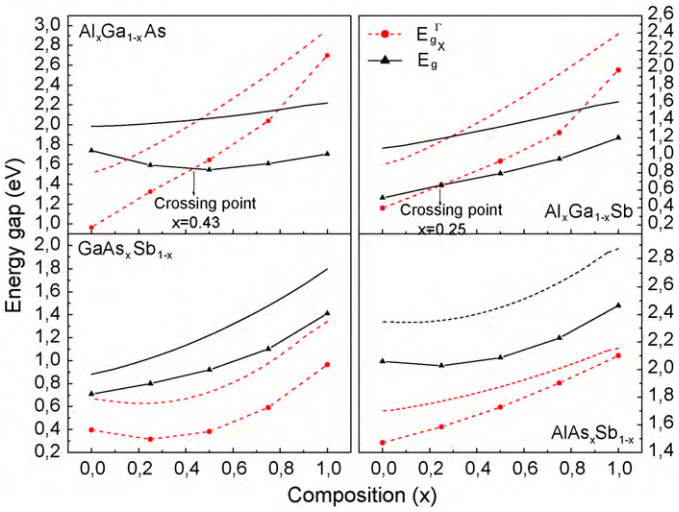


**Fig. 2.** Energy band gap as a function of composition for the ternary alloys. Lines–symbols: calculated values using EV, lines: scissor corrected values.

structures are qualitatively in good agreement with experiments as regards to the ordering of the energy levels and the shape of the bands. Considering this shortcoming of the energy gap, Engel and Vosko constructed a new functional form of the GGA which is able to better reproduce exchange potential at the expense of less agreement in exchange energy. This approach (EV) yields a better band splitting. However, in this method, the quantities that depend on an accurate description of exchange energy $E_x$, such as equilibrium volumes and bulk modulus, are in poor agreement with experiment. Therefore, in order to obtain more accurate energy band gaps in our calculations, we applied EV to the theoretical lattice constants obtained by WC throughout this paper.

The second step of our calculations was to study the structural properties of $Al_xGa_{1-x}As$, $Al_xGa_{1-x}Sb$, $GaAs_xSb_{1-x}$ and $AlAs_xSb_{1-x}$ alloys. Our calculated lattice constants at different compositions, as shown in Fig. 1, were found to vary almost linearly following Vegard's law [37] with a marginal upward bowing parameters equal to −0.008 (Exp. [31]: +0.007 Å), −0.016, −0.098 and −0.099 Å, respectively. However, violation of Vegard's law has been reported in semiconductor alloys both experimentally [38,39] and theoretically [40].

A deviation of the bulk modulus from the linear concentration dependence (see Fig. 1) with downward bowing equal to 0.2 (Exp. [31]: 0.26 GPa), 1.9, 8.4 (Exp. [31]: 19 GPa) and 10.1 GPa for $Al_xGa_{1-x}As$, $Al_xGa_{1-x}Sb$, $GaAs_xSb_{1-x}$ and $AlAs_xSb_{1-x}$ alloys, respectively, was observed. It should be noted that the values of the bulk modulus bowing are small for the two first alloys mainly due to the small contrast in bulk modulus of the constituting binary compounds. A more precise comparison for the behavior of the $GaAs_xSb_{1-x}$ and $AlAs_xSb_{1-x}$ ternary alloys (Fig. 1) shows that a decrease of the lattice constant is accompanied by an increase of the bulk modulus while for the other two ternary alloys the lattice constant increase as well as the bulk modulus. It represents bond strengthening or weakening effects induced by changing the composition.

The crucial role of the four studied ternary alloys in a variety of technologically devices has necessitated precise knowledge of the fundamental energy gap as well as the alignment of the three main conduction-band valleys. Investigations are complicated by the fact that whereas GaSb and GaAs are direct gap materials with $\Gamma$-$L_{-x}$ valley ordering, AlSb and AlAs are indirect gap materials with exactly the reverse ordering. Particular attention has been devoted to the crossover point, at which the $\Gamma$ and X valley minima have the same energies. The EV calculated band gap energy is displayed in Fig. 2. The crossover of direct–indirect gap occurs at $x$ equals to 0.43 (Exp. [31]: 0.45) and 0.25 (Exp. [29]: 0.27) for $Al_xGa_{1-x}As$ and $Al_xGa_{1-x}Sb$ alloys, respectively.

The band gap increases nonlinearly with increasing of the concentration $x$ providing a positive gap bowing. Indeed it is a general trend to describe the band gap of an alloy $AB_xC_{1-x}$ in terms of the pure compound energy gap $E_{AB}$ and $E_{AC}$ by the semi-empirical formula:

$$E_g = xE_{AB} + (1-x)E_{AC} - x(1-x)b, \quad (1)$$

where the curvature $b$ is commonly known as gap bowing parameter.

However one may note that due to the systematic underestimation of the energy band gap in local density approximation (LDA) (GGA)-DFT studies, our results are not accurate enough to be applicable in industry. This obstacle can be overcome by taking into account the scissor correction scheme [41], which in its simplest form requires a rigid shift of the unoccupied part of the DFT-GGA band structure. To do this correction, one may use the experimental values of binary compounds band gaps in Eq. (1) along with the EV calculated band gap bowing parameters. We have done this scissor type correction for all ternary alloys and the results are presented in Fig. 2.

The bowing parameters calculated using Eq. (1) are in reasonable agreement with the corresponding experimental values [42] presented inside the parentheses. The results of $Al_xGa_{1-x}As$, $Al_xGa_{1-x}Sb$, $GaAs_xSb_{1-x}$ and $AlAs_xSb_{1-x}$ alloys are, respectively, equal to 0.455 (0.438), 0.530 (0.47), 1.371 (1.2) and 0.724 (0.691) eV for ($E_g^{\Gamma}$), while for ($E_g^{X}$) they are equal to 0.209 (0.16), 0.202 (0.05), 0.481 (0.31) and 0.322 (0.25) eV.

In order to compute the lattice parameter, bulk modulus, gap energy, refractive index and thermal properties of the $Al_xGa_{1-x}As_ySb_{1-y}$ quaternary alloys we have adopted supercells obtained by a simulated-annealing procedure by which we searched among many 64-atom simple cubic structures, including systems with random, low symmetry, and high symmetry atomic positions, those that minimize the total energy with respect to the cell parameters, and also the atomic positions. We found out that the structure with the most symmetric atomic positions is the most stable system and has the least total energy. Our results concerning lattice constant and bulk modulus are depicted in Figs. 3 and 4, respectively. Accordingly, a marginal deviation of the lattice constant from Vegard's law can be observed. Moreover a large deviation of the bulk modulus from linear concentration dependence is visible.

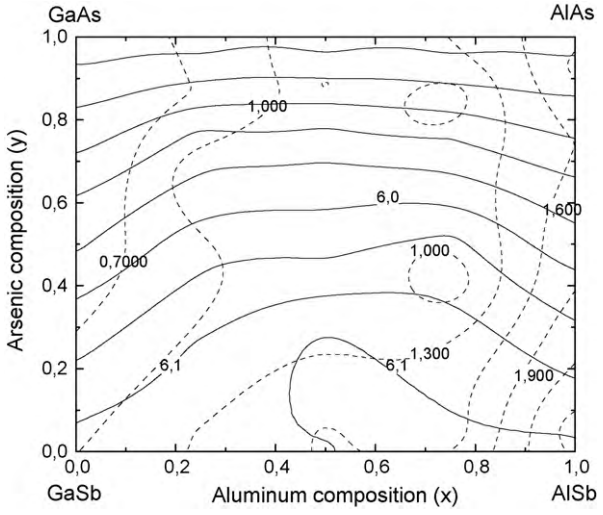


**Fig. 3.** Contour map of the calculated lattice constant in angstroms (solid lines) and direct–indirect minimum energy band gap in electron volts (dashed lines) versus the compositions $x$ and $y$ for $Al_xGa_{1-x}As_ySb_{1-y}$ quaternary alloys.

The formation energies ($E_F$) of quaternary alloys at different concentrations were calculated using the following formula:

$$E_{Form}(x,y) = E_{tot}(x,y) - xyE_{AlAs} + (1-x)yE_{GaAs} + x(1-y)E_{AlSb} + (1-x)(1-y)E_{GaSb}, \quad (2)$$

where $E_{AB}$ is the total energy of the $AB$ binary compounds and $E_{tot}$ is the total energy of quaternary alloys at corresponding concentration. We note that the results of the formation energy do only to some extent provide insight onto stability and for a more complete study the entropy of the system should be included. Fig. 4 shows the results in a contour plot form, the darker part of the graph meaning higher stability of the corresponding alloy. It is apparent that the least stable alloys are those with concentrations near 65% concentration of Al and 60% of As.

The band gap energies of $Al_xGa_{1-x}As_ySb_{1-y}$ alloy were computed using EV and presented in Fig. 3. One can note that the band gap energies depend nonlinearly on the compositions. This figure could be very useful for engineering of semiconductor alloys because it enables us to select alloys with desired optical properties

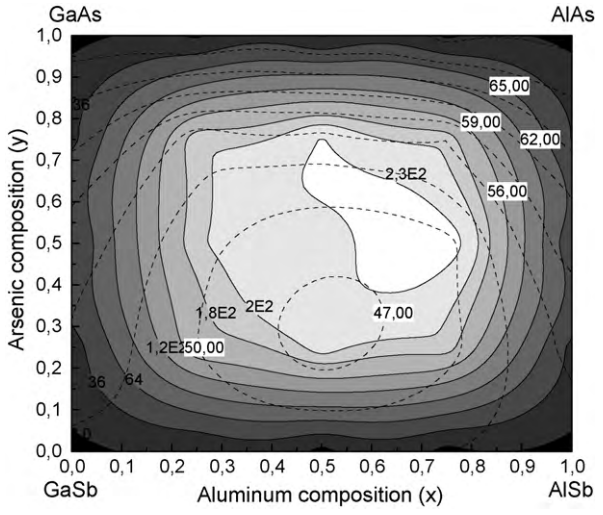


**Fig. 4.** Contour map of the calculated bulk modulus in GPa (dashed lines) and formation energy contour lines in mRyd/pair (solid lines and shadings) versus the compositions $x$ and $y$ for $Al_xGa_{1-x}As_ySb_{1-y}$ quaternary alloys ($E2 = 10^2$).

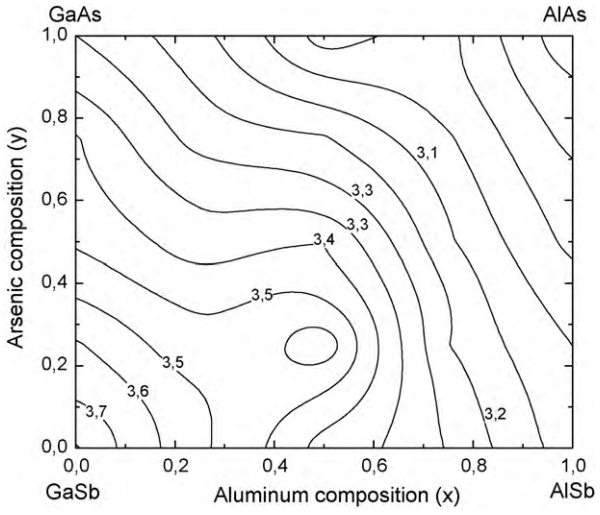


**Fig. 5.** Contour map of the calculated refractive index versus the compositions $x$ and $y$ for $Al_xGa_{1-x}As_ySb_{1-y}$ quaternary alloys.

on any given substrate by looking for concentration in which the system has the required lattice constant and band gap.

The refractive index is known to be one of the most important device parameters because it is strongly connecting with the design of heterostructure lasers, as well as other waveguiding devices. Since the alloys of interest have cubic symmetry, we need to calculate only one dielectric tensor component to completely characterize the linear optical properties. In the following $\varepsilon(\omega)$ is the frequency-dependent dielectric function. The imaginary part $\varepsilon_2(\omega)$ of the frequency-dependent dielectric function is given by [43]

$$\varepsilon_2(\omega) = \frac{e^2\hbar}{\pi m^2\omega^2}\sum_{v,c}\int_{BZ}|M_{cv}(k)|^2\delta[\omega_{cv}(k)-\omega]d^3k. \quad (3)$$

The integral is over the first Brillouin zone, the momentum dipole elements, $M_{cv}(k) = \langle u_{ck} | e.\nabla | u_{vk} \rangle$ where $e$ is the potential vector defining the electric field, are matrix elements for direct transitions between valence band $u_{vk}(k)$ and conduction-band $u_{ck}(k)$ states, and the energy $\hbar\omega_{cv}(k) = E_{ck} - E_{vk}$ is the corresponding transition energy.

The real part $\varepsilon_1(\omega)$ of the frequency-dependent dielectric function can be derived from the imaginary part using the Kramers–Kronig relations:

$$\varepsilon_1(\omega) = 1 + \frac{2}{\pi}P\int_0^\infty \frac{\omega'\varepsilon_2(\omega')}{\omega'^2-\omega^2}d\omega', \quad (4)$$

where $P$ implies the principle value of the integral. Knowledge of both real and imaginary parts of the frequency-dependent dielectric function allows the calculation of important optical functions such as the refractive index $n(\omega)$:

$$n(\omega) = \left[\frac{\varepsilon_1(\omega)}{2} + \frac{\sqrt{\varepsilon_1^2(\omega)+\varepsilon_2^2(\omega)}}{2}\right]^{1/2}. \quad (5)$$

In the calculations of the optical properties, a dense mesh of uniformly distributed $k$ points is required. Hence, the Brillouin zone integration was performed with 816, 729 and 666 $k$ points in the irreducible part of the Brillouin zone for binary, ternary and quaternary compounds, respectively. Broadening is taken to be 0.2 eV. The EV scheme within scissor correction was used in order to perform accurate optical parameter calculations.

Fig. 5 displays the contour map of the calculated refractive index versus the compositions $x$ and $y$ for $Al_xGa_{1-x}As_ySb_{1-y}$ quaternary

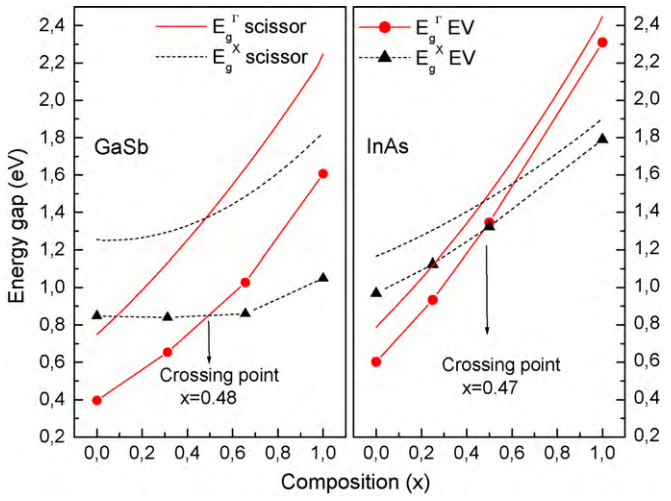


**Fig. 6.** Energy band gap of $Al_xGa_{1-x}As_ySb_{1-y}$ quaternary alloys lattice matched to GaSb and InAs as a function of the $x$ composition. Lines–symbols: calculated values using EV, lines: scissor corrected values.

alloys. One can note that the refractive index decreases with the increasing of $x$ and $y$ and depend nonlinearly on the compositions, especially at around 50% concentration of Al atom and 30% concentration of As atom.

Finally, in order to gain some understanding about the interfaces of our investigated alloys and proximity effects of substrates on them, we present the properties of the $Al_xGa_{1-x}As_ySb_{1-y}$ alloys lattice matched to GaSb and InAs semiconductor substrates. Similar to the ternary alloys, the lattice constant $a(x, y)$ of the quaternary alloy is determined using Vegard's rule as

$$a(x,y) = xya_{AlAs} + (1-x)ya_{GaAs} + x(1-y)a_{AlSb} + (1-x)(1-y)a_{GaSb}, \quad (6)$$

where $a_{AlAs}$, $a_{GaAs}$, $a_{AlSb}$ and $a_{GaSb}$ are the lattice constants of the binary compounds. By putting $a(x, y)$ equal to the lattice constant of GaSb and InAs, the corresponding concentrations for lattice matched $Al_xGa_{1-x}As_ySb_{1-y}$ quaternary alloys are obtained as follows:

For GaSb substrate:

$$y = \frac{0.045x}{0.449 + 0.033x} \quad (0 = x = 1), \quad (7)$$

whereas, for InAs substrate

$$y = \frac{0.015 + 0.045x}{0.449 + 0.033x} \quad (0 = x = 1). \quad (8)$$

The above expression specifies a line on the field of $(x, y)$ concentrations in which the corresponding alloy is lattice matched to the GaSb and InAs substrates. We have considered four different concentrations along the line of lattice matching to both GaAs: $(x, y) = (0/32, 0/32)$; (10/32, 1/32); (21/32, 2/32); (32/32, 3/32) and InAs: $(x, y) = (0/32, 1/32)$; (8/32, 8/32); (16/32, 2/32); (32/32, 4/32). In Fig. 6 we display the energy gap as a function of the aluminum composition along both GaSb and InAs matching lines of the composition. The crossover of direct–indirect gap occurs at $x$ equals to 0.48 (Theor. [13,14]: 0.45) and 0.74 (Theor. [13,14]: 0.45) for lattices matched to GaSb and InAs, respectively. The visible nonlinear behavior of band gap versus concentration $x$ leads to the gap bowing parameters for $E_g^{\Gamma}$ ($E_g^X$) of 0.65 (0.20) and 0.47 (0.22) eV within EV for quaternary alloys lattice matched to GaSb and InAs substrates, respectively. To apply the mentioned scissor type correction to these data, in addition to the bowing parameters, one needs to study the experimental band gaps of the alloys that are at the borders of the lattice matched plots [$(x, y) = (0,0)$; (1,3/32) for matching to GaSb and (0,1/32); (1,1/8) for matching to InAs]. Except for the first one that is a binary alloy, other bordering materials are ternary alloys with no available measured band gap. Therefore instead of the experimental values, we have taken their corrected values from Fig. 2. These parameters were used to apply a similar scissor type correction to the lattice matched data and the results are presented in Fig. 6. The results show that by tuning the concentrations in quaternary alloy, a broad range of band gaps and therefore optical properties are accessible for alloys grown on GaAs and InAs substrates. The EV calculated band gap of $Al_xGa_{1-x}As_ySb_{1-y}$ compound matched to GaSb range from 0.396 to 1.051 eV, while in the case of the InAs substrate, the corresponding range is from 0.602 to 1.789 eV.

**Table 2**
Calculated natural valence band offsets $\Delta E_v$ (eV) of the quaternary alloys lattice matched to GaSb and InAs.

| $x$ | $Al_xGa_{1-x}As_ySb_{1-y}$/GaSb | $x$ | $Al_xGa_{1-x}As_ySb_{1-y}$/InAs |
|---|---|---|---|
| 0 | 0 | 0 | 0.32 |
| 10/32 | 0.02 | 1/4 | 0.41 |
| 21/32 | 0.38 | 1/2 | 0.76 |
| 1 | 0.63 | 1 | 1.12 |

Another property that we have determined from the results of constrained lattice constant calculations is the natural valence band offset $\Delta E_v$ that is defined as the difference between the valence band maximums of two semiconductor compounds forming a heterostructure. As a very important parameter in interfacial structures, it can control several parameters such as quantum confinement of carriers, quality of ohmic contacts, and height of the Schottky barriers. Following Wei and Zunger [44] the valence band offset between compounds $AX$ and $BY$ is given by

$$\Delta E_v\left(\frac{AX}{BY}\right) = \Delta E_{v,C'}^{BY} - \Delta E_{v,C}^{Ax} + \Delta E_{C,C'}^{AX/BY}, \quad (9)$$

where $\Delta E_{v,C}^{Ax} = E_v^{AX} - E_C^{AX}$ (and similarly for $\Delta E_{v,C'}^{BY}$) are the core level ($C$) to valence band maximum separation for pure $AX$ (pure $BY$), while $\Delta E_{C,C'}^{Ax/BY} = E_{C'}^{BY} - E_C^{AX}$ is the difference in core level binding energy between $AX$ and $BY$ at the $AX/BY$ heterojunction. Therefore accurate description of $\Delta E_v\left(\frac{AX}{BY}\right)$ needs the $AX/BY$ heterojunction calculations that for a quaternary alloy could be a very heavy task. However, the results obtained using Eq. (9) show that band offset is indeed a bulk property and could be calculated with reasonable accuracy using bulk values [44]

$$\Delta E_v\left(\frac{AX}{BY}\right) = \Delta E_v^{BY} - \Delta E_v^{AX} \quad (10)$$

We have used this formula for reliable estimation of $\Delta E_v$ for $Al_xGa_{1-x}As_ySb_{1-y-y}$/GaSb and $Al_xGa_{1-x}As_ySb_{1-y}$/InAs heterostructures. Our calculated valance band offsets that are presented in Table 2, show a monotonic increase of $\Delta E_v$ versus concentration for both GaSb and InAs semiconductor substrates. It is clearly seen that the offsets could be varied in a broad range by changing the concentrations, thus indicating high susceptivity of $Al_xGa_{1-x}As_ySb_{1-y}$ for band engineering and designing heterostructures with the desired interfacial properties.

The calculated refractive indices of the lattice matched systems as a function of photon energy are shown in Fig. 7. One can conclude that the refractive index of $Al_xGa_{1-x}As_ySb_{1-y}$ alloys decreases with increasing of the composition $x$ in both case, lattice matched GaSb and InAs. The calculated refractive index of $Al_xGa_{1-x}As_ySb_{1-y}$ compound matched to GaSb range from 3.83 to 3.38 while in the case of the InAs substrate, the corresponding range is from 4.07 to 3.18.

Finally, to investigate some thermal properties, we used the quasi-harmonic Debye model [45] in which the non-equilibrium

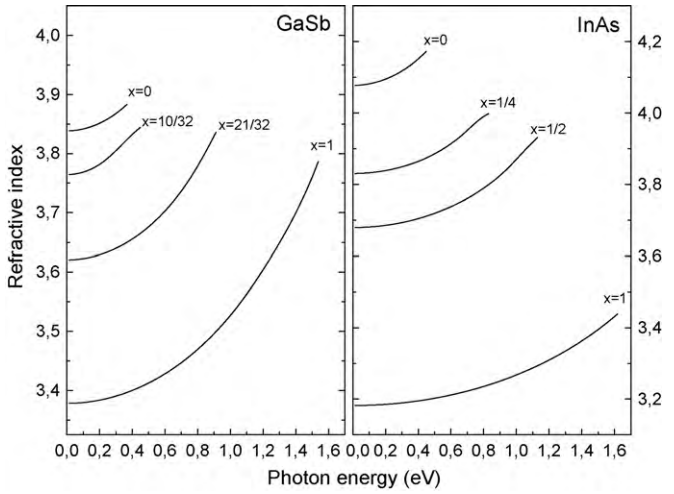


**Fig. 7.** Calculated refractive indices of $Al_xGa_{1-x}As_ySb_{1-y}$ quaternary alloys lattice matched to GaSb and InAs.

Gibbs function $G^*(V; P, T)$ is written in the form:

$$G^*(V; P, T) = E(V) + PV + A_{vib}[\theta(V); T], \tag{11}$$

where $E(V)$ is the total energy per unit cell, $PV$ corresponds to the constant hydrostatic pressure condition, $\theta(V)$ is the Debye temperature and $A_{vib}$ is the vibrational term which can be written using the Debye model of the phonon density of states as:

$$A_{vib}(\theta; T) = nkT\left[\frac{9\theta}{8T} + 3\ln(1 - e^{-\theta/T}) - D\left(\frac{\theta}{T}\right)\right], \tag{12}$$

where $n$ is the number of atoms per formula unit, $D(\theta/T)$ represents the Debye integral and for an isotropic solid, $\theta$ is expressed as:

$$\theta_D = \frac{\hbar}{k}\left[6\pi^2 V^{1/2} n\right]^{1/3} f(\sigma)\sqrt{\frac{B_S}{M}}, \tag{13}$$

$M$ being the molecular mass per unit cell and $B_S$ the adiabatic bulk modulus, approximated by the static compressibility:

$$B_S \cong B(V) = V\frac{d^2E(V)}{dV^2}. \tag{14}$$

Details on $f(\sigma)$ can be found elsewhere [46,47]. Therefore, the non-equilibrium Gibbs function $G^*(V; P, T)$ as a function of $V$, $P$ and $T$ can be minimized with respect to volume $V$:

$$\left[\frac{\partial G^*(V; P, T)}{\partial V}\right]_{P,T} = 0. \tag{15}$$

By solving Eq. (15), one can obtain the thermal equation-of-state (EOS) $V(P, T)$. The heat capacity $C_V$ and the thermal expansion coefficient $\alpha$ are given by [48]:

$$C_V = 3nk\left[4D\left(\frac{\theta}{T}\right) - \frac{3\theta/T}{e^{\theta/T} - 1}\right], \tag{16}$$

$$\alpha = \frac{\gamma C_V}{B_T V}, \tag{17}$$

where $\gamma$ is the Grüneisen parameter defined as

$$\gamma = -\frac{d\ln\theta(V)}{d\ln V}. \tag{18}$$

Through the quasi-harmonic Debye model, one could calculate the thermodynamic quantities of any temperatures and pressures of compounds from the calculated $E$–$V$ data at $T = 0$ and $P = 0$.

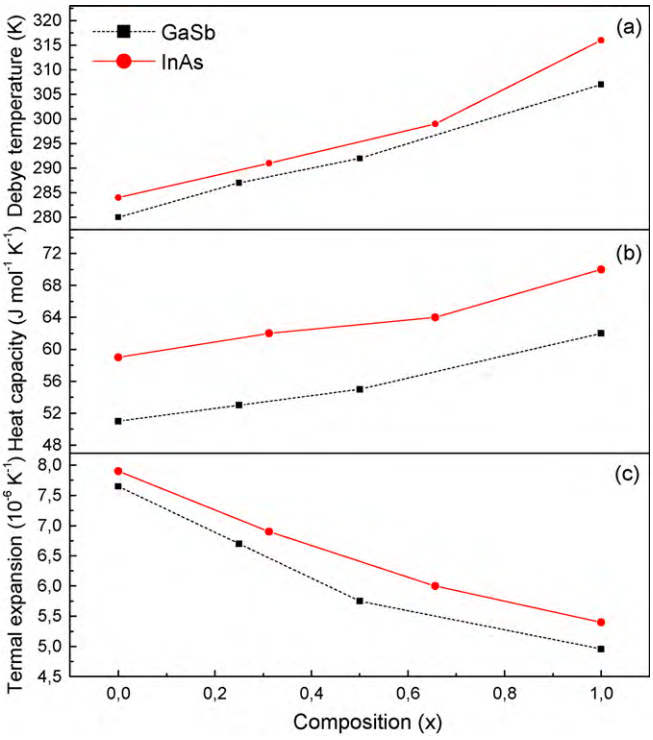


**Fig. 8.** The thermal properties of $Al_xGa_{1-x}As_ySb_{1-y}$ quaternary alloys lattice matched to GaSb and InAs: (a) the Debye temperature $\theta$, (b) the heat capacity $C_V$ and (c) the thermal expansion $\alpha$.

Fig. 8 displays the Debye temperature $\theta$, the heat capacity $C_V$ and the thermal expansion $\alpha$ at room temperature of $Al_xGa_{1-x}As_ySb_{1-y}$ quaternary alloys lattice matched to GaSb and InAs. The increase of concentration $x$ leads to the Debye temperature increase as well as the compressibility decrease. This result is in accordance with the fact that Debye temperature is proportional to the bulk modulus and that a hard material exhibits a high Debye temperature. It should be noted that the variation of the three thermal parameters as a function of concentration is not linear.

## 4. Conclusions

We have investigated the structural and electronic properties of the quaternary $Al_xGa_{1-x}As_ySb_{1-y}$ and their four pseudobinary alloys as a function of the compositions $x$ and $y$ using the FP-LAPW method within DFT. A nonlinear behavior of the lattice constant, bulk modulus and band gap dependence on $x$ and $y$ has been observed. The calculations of formation energies showed that the least stable alloys are around 65% concentration of Al atom and 60% concentration of As atom. Our results regarding the gap bowing of the ternary alloys are found to be in reasonable agreement with the experimental data. The crossover of direct–indirect gap occurs at $x$ equals to 0.43 and 0.25 for $Al_xGa_{1-x}As$ and $Al_xGa_{1-x}Sb$ alloys, respectively. The energy band gap, the offset, the refractive index and the thermal properties of the quaternary alloys $Al_xGa_{1-x}As_ySb_{1-y}$ matching to GaSb and InAs substrates have been investigated.

## Acknowledgments

One of the authors (F.H.H.) would like to thank the Doctoral School of Sciences and Technology in the Lebanese university (EDST), Abdus Salam International Centre for Theoretical Physics (ICTP) and Metz University for their financial support during the realization of this work.

## References


[1] U.K. Mishra, J. Singh, Semiconductor Device Physics and Design, Springer, Dordrecht, 2008.
[2] M. Othman, E. Kasap, N. Korozlu, J. Alloys Compd. 496 (2010) 226.
[3] (a) K. Iga, S. Kinoshita, Process Technology for Semiconductor Lasers, Springer-Verlag, Berlin, 1996;
(b) M. Quillec, Materials for Optoelectronics, Kluwer Academic Publ., Boston, 1996.
[4] R.E. Nabory, M.A. Pollack, E.D. Beebe, J.C. Dewinter, R.W. Dixon, Appl. Phys. Lett. 28 (1976) 19.
[5] A. Sasaki, M. Nishimura, Y. Takeda, Jpn. J. Appl. Phys. 19 (1980) 1965.
[6] (a) M. Dolginov, A.E. Drakin, L.V. Druzhinina, P.G.M.G. Milvidsky, V.A. Skripkin, B.N. Sverdlov, IEEE J. Quantum Electron. QE-17 (1981) 593;
(b) T.P. Pearsall, R.E. Nahory, M.A. Pollack, Appl. Phys. Lett. 28 (1976) 403.
[7] M.L. Timmons, S.M. Bedair, R.J. Markunas, J.A. Hutenby, Proceedings of the Conf. Record. 16th IEEE Photovoltaic Specialists Conference IEEE, New York, 1982, p. 663.
[8] E.A. Montie, P.J.A. Thijis, G.W. Hooft, Appl. Phys. Lett. 53 (1988) 1611.
[9] K.Y. Lau, S. Xin, W.I. Wang, N. Bar-Chaim, M. Mittelistein, Appl. Phys. Lett. 55 (1988) 1173.
[10] H. Ait Kaci, D. Boukredimi, M. Mebarki, Phys. Status Solidi A 163 (1997) 101.
[11] S.H. Wang, S.E. Mohney, J.A. Robinson, Semicond. Sci. Technol. 20 (2005) 755.
[12] F. El Haj Hassan, A. Breidi, S. Ghemid, B. Amrani, H. Meradji, O. Pagès, J. Alloys Compd. 499 (2010) 80.
[13] S. Adachi, J. Appl. Phys. 61 (1987) 4869.
[14] S. Adachi, J. Appl. Phys. 58 (1985) R1.
[15] K. Shim, Solid State Commun. 134 (2005) 437.
[16] M. Rabah, H. Abid, B. Bouhafs, H. Aourag, Mater. Chem. Phys. 74 (2002) 328.
[17] N. Bouarissa, R. Bachiri, Mater. Chem. Phys. 78 (2002) 271.
[18] A. Zunger, S.-H. Wei, L.G. Ferreira, J.E. Bernard, Phys. Rev. Lett. 65 (1990) 353.
[19] D.D. Koelling, B.N. Harmon, J. Phys. C: Solid State Phys. 10 (1977) 3107.
[20] G.K.H. Madsen, P. Blaha, K. Schwarz, E. Sjöstedt, L. Nordström, Phys. Rev. B 64 (2001) 195134.
[21] K. Schwarz, P. Blaha, G.K.H. Madsen, Comput. Phys. Commun. 147 (2002) 71.
[22] P. Hohenberg, W. Kohn, Phys. Rev. 136 (1964) 864.
[23] W. Kohn, L.J. Sham, Phys. Rev. A 140 (1965) 1133.
[24] P. Blaha, K. Schwarz, G.K.H. Madsen, D. Kvasnicka, J. Luitz, WIEN2K "an augmented plane wave + local orbitals program for calculating crystal properties", Karlheinz Schwarz, Techn. Universitat, Wien, Austria, 2001, ISBN 3-9501031-1-2.
[25] Z. Wu, R.E. Cohen, Phys. Rev. B 73 (2006) 235116.
[26] J.P. Perdew, K. Burke, M. Ernzerhof, Phys. Rev. Lett. 77 (1996) 3865.
[27] E. Engel, S.H. Vosko, Phys. Rev. B 47 (1993) 13164.
[28] F.D. Murnaghan, Proc. Natl. Acad. Sci. USA 30 (1944) 244.
[29] I. Vurgaftman, J.R. Meyer, L.R. Ram-Mohan, J. Appl. Phys. 89 (2001) 5815.
[30] K. Strössner, S. Ves, C.K. Kim, M. Cardona, Phys. Rev. B 33 (1986) 4044.
[31] M. Levinshtein, S. Rumyantsev, M. Shur, Handbook Series on Semiconductor Parameters, vol. 2, Ternary and Quaternary III–V Compounds, World Scientific, 1999.
[32] F. El Haj Hassan, B. Amrani, J. Phys.: Condens. Matter. 19 (2007) 386234.
[33] F. El Haj Hassan, H. Akbarzadeh, Comput. Mater. Sci. 35 (2006) 423.
[34] P. Dufek, P. Blaha, K. Schwarz, Phys. Rev. B 50 (1994) 7279.
[35] F. El Haj Hassan, S.J. Hashemifar, H. Akbarzadeh, Phys. Rev. B 73 (2006) 195202.
[36] F. El Haj Hassan, H. Akbarzadeh, S.J. Hashemifar, J. Phys.: Condens. Matter. 16 (2004) 3329.
[37] L. Vegard, Z. Phys. 5 (1921) 17.
[38] B. Jobst, D. Hommel, U. Lunz, T. Gerhard, G. Landwehr, Appl. Phys. Lett. 69 (1996) 97.
[39] J.P. Dismuckes, L. Ekstrom, R.J. Poff, J. Phys. Chem. 68 (1964) 3021.
[40] F. El Haj Hassan, H. Akdarzadeh, Mater. Sci. Eng. B 121 (2005) 170.
[41] V. Fiorentini, A. Baldereschi, Phys. Rev. B 51 (1995) 17196.
[42] O. Madelung, Semiconductors Basic Data, Springer, Berlin, 1996.
[43] C. Amrosch-Draxl, J.O. Sofo, Comput. Phys. Commun. 175 (2006) 1.
[44] S.-H. Wei, A. Zunger, Appl. Phys. Lett. 72 (1998) 2011.
[45] M.A. Blanco, E. Francisco, V. Luaña, Comput. Phys. Commun. 158 (2004) 57.
[46] E. Francisco, J.M. Recio, M.A. Blanco, A. Martín Pendás, J. Phys. Chem. 102 (1998) 1595.
[47] E. Francisco, M.A. Blanco, G. Sanjurjo, Phys. Rev. B 63 (2001) 094107.
[48] R. Hill, Proc. Phys. Soc. Lond. A 65 (1952) 349.